*Chem Biol Drug Des 2016*

Research Article

# Antibacterial Activity of Imidazolium-Based Ionic Liquids Investigated by QSAR Modeling and Experimental Studies

**Diana Hodyna[1,*], Vasyl Kovalishyn[1], Sergiy Rogalsky[2], Volodymyr Blagodatnyi[3], Kirill Petko[4] and Larisa Metelytsia[1]**

*[1]Department of Medical and Biological Researches, Institute of Bioorganic Chemistry and Petrochemistry, NAS of Ukraine, 1, Murmanska Street, Kyiv 02160, Ukraine*
*[2]Laboratory of Modification of Polymers, Institute of Bioorganic Chemistry and Petrochemistry, NAS of Ukraine, 50, Kharkivske Schose, Kyiv 02160, Ukraine*
*[3]Department of Microbiology and Epidemiology, Shupyk National Medical Academy of Postgraduate Education, 9, Dorogozhytska Street, Kyiv 04112, Ukraine*
*[4]Organofluorine Compounds Chemistry Department, Institute of Organic Chemistry, NAS of Ukraine, 5, Murmanska Street, Kyiv 02660, Ukraine*
**Corresponding author: Diana Hodyna, dianahodyna@gmail.com*

**Predictive QSAR models for the inhibitors of *B. subtilis* and *Ps. aeruginosa* among imidazolium-based ionic liquids were developed using literary data. The regression QSAR models were created through Artificial Neural Network and *k*-nearest neighbor procedures. The classification QSAR models were constructed using WEKA-RF (random forest) method. The predictive ability of the models was tested by fivefold cross-validation; giving $q^2$ = 0.77–0.92 for regression models and accuracy 83–88% for classification models. Twenty synthesized samples of 1,3-dialkylimidazolium ionic liquids with predictive value of activity level of antimicrobial potential were evaluated. For all asymmetric 1,3-dialkylimidazolium ionic liquids, only compounds containing at least one radical with alkyl chain length of 12 carbon atoms showed high antibacterial activity. However, the activity of symmetric 1,3-dialkylimidazolium salts was found to have opposite relationship with the length of aliphatic radical being maximum for compounds based on 1,3-dioctylimidazolium cation. The obtained experimental results suggested that the application of classification QSAR models is more accurate for the prediction of activity of new imidazolium-based ILs as potential antibacterials.**

**Key words:** antibacterial activity, imidazolium ionic liquids, QSAR

Received 1 December 2015, revised 11 March 2016 and accepted for publication 28 March 2016

The development of antibiotic resistant bacteria, especially biofilm-forming variants, is becoming a serious threat in human society since they cause numerous health care-associated infections (1,2). In some cases the resistance of bacterial biofilms against antibiotics can be increased up to 1000-fold compared to isolated colonies (2). Research in alternative biocides with decreased potential for resistance development is therefore topical nowadays.

Cationic antimicrobials have been in general use within clinical and domestic settings for over half a century. Amongst the most useful antiseptics and disinfectants are the quaternary ammonium compounds (cetrimide, benzalkonium chloride), cetylpyridinium chloride, bisbiguanides (chlorhexidine), and polymeric biguanides (3). However, the use of such antimicrobial agents has been questioned in many application areas due to the narrowed spectrum of their activity, as well as growing problems associated with the development and spread of bacterial resistance (3–5). Thus, conventional quaternary ammonium-based antimicrobials, as well as chlorhexidine showed low efficacy against Gram-negative bacteria (3,5–7).

Over recent years ionic liquids (ILs), which are low-temperature molten salts entirely consisting of discrete cations and anions, have attracted growing interest as extremely promising new class of 'green' chemicals (8). Due to the unique combination of negligible vapor pressure, non-flammability, and low toxicity, as well as high solvency for a broad range of organic and inorganic compounds, ILs have found numerous applications such as alternative 'green' solvents in organic synthesis and liquid–liquid extractions (8), polymer chemistry (9), enzyme catalysis (10,11), drug delivery systems (12) etc. Overall, the ability to 'tune' the physical, chemical, and biological properties of ILs by modification of the properties of the constituent of cations and anions create enormous potential for their industrial use (13).

Many researchers have examined the antimicrobial potency of different ILs, comprising imidazolium, pyridinium, pyrrolidinium cations and various anions against

 doi: 10.1111/cbdd.12770

the gram-positive and gram-negative bacteria, including biofilm-forming bacteria, and fungi (13–22). Most widely studied ILs comprise asymmetric 1-alkyl-3-methylimidazolium cations and small inorganic anions (14–16,20–23). ILs with long alkyl chain substituents have structural similarity with conventional quaternary ammonium based surfactants comprising positively charged hydrophilic head group and hydrophobic tail which therefore gives them an inherent amphiphilic nature (3,22,23). It has been found that biological activity of imidazolium based ILs is closely related to their surfactant properties and therefore greatly affected by the cation alkyl side chain length, whereas the type of anion has little effect on their activity (14,22,23). Among the homologous investigated, ILs with an alkyl chain length of 12 and 14 carbon atoms showed the highest efficiency as antimicrobial agents (22,23). The mechanism of antimicrobial action of ILs is considered similar to those reported for cationic surfactants which interact with phospholipid components in the cytoplasmic membrane resulting in a deformation of membrane permeability and lethal leakage of cytoplasmic materials (3,24). However, in comparison with conventional quaternary ammonium biocides, long-chain imidazolium based ILs were found to possess much broader range of antimicrobial activity against Gram-negative and Gram-positive bacteria and fungi (15,23). Moreover, 1-alkyl-3-methylimidazolium ILs showed strong antibiofilm activity against a panel of pathogen micro-organisms (13,21). Thus, ILs are promising candidates for further development of new antimicrobial agents with much broader application area.

It should be noted that ILs based on symmetric 1,3-dialkylimidazolium cations are practically not been studied for biological activity. However, these compounds also seem very promising primarily due to their lower cost and simplicity of the synthesis.

Overall, the increasing quantity of ILs with a huge number of a combination of different cations and anions increases formed the problem of creation of computer expert systems for a prediction of the properties of new ILs, in especially the bactericidal properties.

Now a number of QSAR models for a prediction of the ILs physical and chemical properties is known. Predicting the biological properties of ILs is not a standard procedure due to a limited number of research results, their unification and due to the difficulties of representation of their structural features as objects for the predicting.

In the present work we offer effective QSAR models for the prediction of antibacterial activity of a number of imidazolium based ILs, comprising both symmetric and asymmetric 1,3-dialkylimidazolium cations, and experimental studies of their activity as potential antibacterial agents.

## Materials and Methods

### *Data set*

The databases for our analysis were retrieved from the literature and stored in the Online Chemical Modeling environment (OCHEM)a in Excel format. The biological data obtained as minimum inhibitory concentration (MIC) were converted into log (1/MIC) values and used as dependent variable in the following QSAR studies. Structural formulas of ILs were drawn using MarvinSketch and imported in SMILES format. The data set consisted of 47 *B. subtilis* inhibitors (*dataset 1*) and 83 *Ps. aeruginosa* inhibitors (*dataset 2*). The range of MIC values of the 83 ILs was from 1.1 to 8600 mkg/mL and of 47 ILs from 0.3 to 1443 mkg/mL. The OCHEM allows using conditions of experiments in the modeling process as descriptors, that's why the basic characteristic of ILs such as a type of anion was used as obligatory condition for properties in OCHEM.

### *Machine learning methods*

In this study, we used the OCHEM to develop high accuracy models for predicting antibacterial activity of imidazolium-based ILs. Several machine-learning methods were used to build QSAR models **-** Associative Neural Network (ASNN) and k-nearest neighbor Method (k-NN) for creating of the regression models and WEKA-RF – for classification models.

### Associative neural network

An associative neural network (ASNN) is an ensemble-based method inspired by the function and structure of neural network correlations in brain. The method operates by simulating the short- and long-term memory of neural networks. The long-term memory is represented by ensembling of neural network weights, while the short-term memory is stored as a pool of internal neural network representations of the input pattern. It allows the ASNN to incorporate new data cases in short-term memory and provides high generalization ability without the need to retrain the neural network weights (25).

This method uses the correlation between ensemble responses (each molecule is represented in the space of neural network models as a vector of predictions of neural network models) as a measure of distance amid the analyzed cases for the nearest neighbor technique. Thus, ASNN performs k-NN in the space of ensemble predictions. It provides an improved prediction by the bias correction of the neural network ensemble. The k-NN method was used for correction of predicted values averaged over an ensemble of neural networks based on errors in prediction of k-nearest neighbors in chemical space or in space of an ensemble of Back Propagation Neural Network (BPNN) models. This process of correcting predicted values based on a set of nearby patterns is targeted to diminish the systematic error for a subset of chemical

space and known as Local Correction (LC) or Associative Memory approach (26).

### *k*-Nearest neighbor method

K-Nearest Neighbors predicts the property (activity) using the average property value of those *k* compounds from the training set that are the nearest (in the descriptor space) to the target compound. The configurable options are: metrics type (Euclidean distance) and the number of neighbors. The optimal value of *k* in the range of 1–100 was automatically detected by OCHEM (27).

### WEKA-RF (random forest)

The random forest machine learner meaning consisting of many individual learners (trees). The random forest uses multiple random trees classifications to votes on an overall classification for the given set of inputs. In general, in each individual machine learner vote is given equal weight (28). RF is a combination of tree predictors such that each tree depends on the values of a random vector sampled independently and with the same distribution for all trees in the forest. Random inputs and random features produce good results in classification. This is a high-dimensional non-parametric method that works well on large numbers of variables (29).

### Descriptors

The descriptors were calculated using six descriptor packages, which cover different representations of chemical structures from simple type of descriptors and a count of chemical groups, to packages offering a wide variety of descriptors types, such as E-State indices, ALogPS, ADRIANA.Code, Dragon V6.0, Chemaxon, Inductive descriptors available in the OCHEM.

*ALogPS* (2D) descriptors were used as parameters of lipophilicity (logP) and water solubility of chemical compounds. The AlogP estimates are provided only for compounds having C, H, O, N, S, Se, P, B, Si, and halogens (30).

*E-State indices* (2D) are separated on atom/bond type, which were attracted atom indices, atom and bonds counts. E-State indices combine the electronic character and the topological environment of each skeletal atom (31).

*ADRIANA.Code* (3D) comprises a unique combination of methods for calculating molecular descriptors on a sound geometric and physicochemical basis. Thus, they are all prone to an interpretation and allow the understanding of the influence of various structural and physicochemical effects on the property under investigation.b ADRIANA.-Code descriptors includes global molecular descriptors (molecular weight, topological polar surface area, molecular dipole moment, number of atoms, number of rotatable bonds, molecular and ring complexity, number of hydrogen bonding acceptors and donors) and spatial or 3D property-weighted autocorrelation descriptors (charge, electronegativity, and others)

*Dragon V6.0* descriptors (3D) include more than 4885 descriptors organized into 29 different logical blocks. Among them, we have selected the following types of descriptors: topological indices, information indices, drug-like indices, ring descriptors, functional group counts, walk and path counts, atom-centered fragments, molecular properties.c

*Chemaxon descriptors*, including elemental analysis, charge, geometry, and others were used to calculate a range of physical, chemical and life-science related properties from chemical structures.d

*Inductive descriptors* (3D) were computed for bound atoms, groups and molecules using intramolecular distances, atomic electro-negativities, charge and covalent radii (32).

### Descriptors selection

Unsupervised filtering of descriptors was applied to each descriptor set before using it as a machine learning input. Before the development of QSAR models, descriptors, which contained of two or fewer non-zero values for the whole training set were eliminated. Besides, descriptors which were inter-correlated with a linear correlation coefficient of $R^2 > 0.95$ were batched together and only one descriptor from the group was taken for development of QSAR model. This unsupervised filtering does not use any information about the biological activity and thus does not introduce selection bias (33), which could provide chance correlations.

### Validation of QSAR models

The accuracy of all individual models was evaluated using the fivefold cross-validation (CV) procedure. In the fivefold cross-validation the initial data set was divided into five subsets of approximately equal size. Each QSAR model was built using 4/5 of the compounds from the initial training set. The remaining 20% of compounds were predicted and were used to estimate the model accuracy. This procedure was sequentially repeated five times producing five different external validation data sets and corresponding training set molecules.e These predictions were used to estimate the CV validity of the model. Then the average statistical coefficients for all five-test sets were computed by OCHEM.

### Statistical coefficients

### Classification models

The OCHEM server uses the average correct classification rate (in percents) as a measure of classification models

quality. The correct classification rate is complemented with a confusion matrix that shows a number of compounds classified correctly for every class as well as details of misclassified compounds, e.g. how many compounds from the class A are classified to belong to the class B. We used the most common case of classification models - binary classification, where the instances belong to either active or inactive class. To assess the classification ability the following statistical measures which are applicable to binary classification models: accuracy (percentage of correctly classified samples), class hit rate – sensitivity for active tasks class and specificity for inactive class, precision – active and inactive predictive value were calculated.

### Regression models

Regression models were evaluated with the cross-validation coefficient, $q^2$. The prediction performance of the methods was compared using the root mean squared error (RMSE), mean absolute error (MAE), and squared correlation coefficient, $R^2$.f

QSAR models are considered effective at the value of $R^2 > 0.6$ and $q^2 > 0.5$ and can be used to assess the activity of new compounds (34).

### *Applicability domain*

Each QSAR model should have an applicability domain (AD) since the model could only cover a limited range of the entire chemical space. AD was determined for each model to avoid incorrect predictions. A unique feature of the OCHEM is the automatic assessment of the prediction accuracy. The estimation of the accuracy is based on the concept of 'distance to a model', (DM) (35) i.e. some numeric value is estimated solely from molecular structures and experimental conditions, which correlates with the average model performance. In the current study, we used the standard deviation of predictions of the ensemble of the regression models in the bagging approach (BAGGING-STD) or in a consensus model (CONSENSUS-STD) as a measure to distinguish reliable and non-reliable predictions under the OCHEM.g

As result, OCHEM automatically detects AD for each new molecule (i.e. whether a molecule inside or outside of AD) for current QSAR model.

### *Antimicrobial activity of 1,3-dialkylimidazolium ionic liquid*

The method of disc diffusion in Mueller-Hinton agar (36) was used for testing antibacterial activity of imidazolium-based ionic liquids against gram-positive *B. subtilis* ATCC 6633 and gram-negative *Ps. aeruginosa* ATCC 27853. Zones of inhibition were formed by testing compounds under condition of microbial loading $1 \times 10^5$ colony forming units (CFU) in 1 mL. About 0.02 mL of the tested compounds applied on standard paper discs. All compounds were tested at identical concentrations 1% and 0.1% and were presented on a disc in moles respectively. The compounds which formed zones of growth inhibition of microbes ≥15 mm were accepted as active.

## Results and Discussion

### *Statistical results of QSAR modeling*

Classification and regression QSAR models for predicting antimicrobial activity of imidazolium-based ILs was created in the search for potential new *Ps. aeruginosa* and *B. subtilis* inhibitors. In preprocessing steps using ChemAxon Standardizerd all structures were standardized and then optimized with Corina.h

### *Classification models*

Two QSAR models were developed by the WEKA-RF method using the ALogPS, E-State indices, ADRIANA.Code, Dragon V6.0, Inductive descriptors and Type of anion. Before creating QSAR models, the numerical values (MIC) were discretized so that 50% of the compounds were considered active and 50% inactive. The results on classification models of antibacterial activity of ILs against *B. subtilis* and *Ps. aeruginosa* are summarized in Table 1.

The percentage of correctly classified samples (Accuracy) for classification QSAR models of antibacterial imidazolium-based ILs with activity against *B. subtilis* and *Ps. aeruginosa* was 83% and 88% respectively (Table 1).

### *Regression models*

To improve the accuracy of predicted results of classification QSAR models four regression QSAR models were created using ASNN method including ALogPS, E-State indices, ADRIANA.Code, Dragon V6.0, Chemaxon, Inductive descriptors, Type of anion and one model using *k*-NN method including ALogPS, E-State, Type of anion descriptors. The predicted activity for tests molecules using a consensus model was calculated as a usual conditionally weighted average from predictions of all five models.

**Table 1:** Comparison of parameters of classification QSAR models of antibacterial imidazolium ILs with activity against *B. subtilis* (*dataset 1*) and *Ps. aeruginosa* (*dataset 2*) by WEKA-RF method

| Parameters | *dataset 1* | *dataset 2* |
|---|---|---|
| Number of descriptors | 191 | 146 |
| Precision (active) | 0.81 | 0.86 |
| Precision (inactive) | 0.86 | 0.90 |
| Sensitivity | 0.88 | 0.90 |
| Specificity | 0.79 | 0.86 |
| Accuracy | 83% ± 5.0 | 88% ± 4.0 |

**Table 2:** Molecular descriptors of QSAR models of antibacterial activity

| Model | Method | Types of descriptors | Number of descriptors |
|---|---|---|---|
| 1 | ASNN | ALogPS<br>E-State indices<br>Type of anion | 14–18 |
| 2 | ASNN | ADRIANA.Code<br>Type of anion | 63 |
| 3 | ASNN | Chemaxon<br>Type of anion | 37 |
| 4 | ASNN | Dragon V6.0<br>Inductive descriptors<br>Type of anion | 114 |
| 5 | *k*-NN | ALogPS<br>E-State indices<br>Type of anion | 18 |

The methods, types and number of descriptors by each studied micro-organism are presented in the Table 2.

## Results of QSAR modeling for *B. subtilis* inhibitor (*dataset 1*)

Table 3 summarizes the statistical parameters of the regression QSAR models for *dataset 1.* According to the statistical significance presented in Table 3, the cross-validation coefficient $q^2$ for all models ranged from 0.77 to 0.86, confirms their high predictive ability. The correlation between the observed and predicted values log(MIC) of the consensus QSAR model for *dataset 1* is given graphically in Figure 1.

The graphically results reported in Figure 1 show that the difference between experimental and predicted values of the activity of imidazolium ILs against *B. subtilis* (*dataset 1*) does not exceed 0.9 log units for all compounds with a high cross-validation coefficient $q^2 = 0.86$ and low MAE (MAE = 0.34).

## Results of QSAR modeling for *Ps. aeruginosa* inhibitor (*dataset 2*)

Statistical parameters of the regression QSAR models for *dataset 2* are presented in Table 4. According to the statistical parameters presented in Table 4, the QSAR models of activity of imidazolium ILs as inhibitors of *Ps. aeruginosa* (*dataset 2*) are stable and predictive both internally, verified by the statistical parameters (high value of cross-validation parameters $q^2 = 0.81$–$0.92$ and low MAE = 0.18–0.24). The results of the correlation between the observed and predicted values log(MIC) of the consensus QSAR model for *dataset 2* are presented graphically in Figure 2.

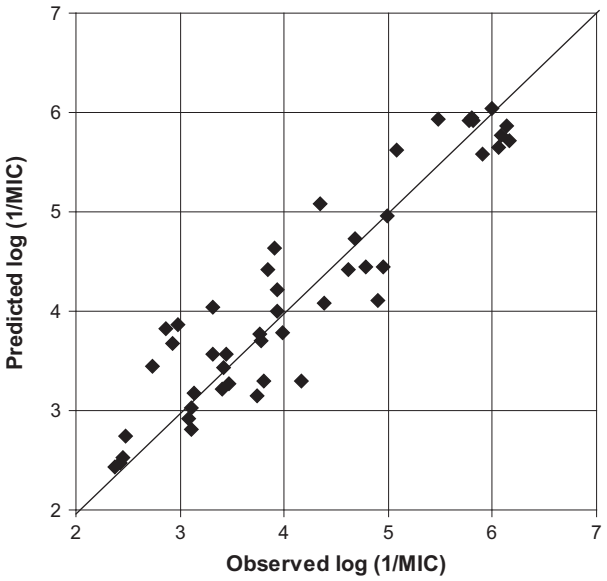


**Figure 1:** Plots of experimental values and predicted values of the consensus QSAR model for *dataset 1*.

After analyzing the prediction results for all compounds of this dataset, we found that all compounds except one compound are well-predicted with smaller residues lower than 1 log unit (Figure 2). The total accuracy $q^2$ of the consensus QSAR model of antibacterial activity of ILs against *Ps. aeruginosa* (*dataset 2*) was about 0.91, MAE = 0.18.

As it can be seen from the Tables 1, 3 and 4, the predictive ability of classification models and regression models is high. Twenty structures of 1,3-dialkylimidazolium ionic

**Table 3:** Statistical coefficients of QSAR models for *dataset 1*

| | Statistical coefficients | | | |
|---|---|---|---|---|
| QSAR Models | $q^2$ | $R^2$ | RMSE | MAE |
| Model 1 | 0.86 ± 0.04 | 0.86 ± 0.04 | 0.43 ± 0.04 | 0.34 ± 0.04 |
| Model 2 | 0.84 ± 0.05 | 0.85 ± 0.04 | 0.46 ± 0.05 | 0.35 ± 0.04 |
| Model 3 | 0.85 ± 0.04 | 0.86 ± 0.04 | 0.44 ± 0.04 | 0.35 ± 0.04 |
| Model 4 | 0.84 ± 0.04 | 0.84 ± 0.04 | 0.47 ± 0.04 | 0.38 ± 0.04 |
| Model 5 | 0.77 ± 0.07 | 0.79 ± 0.06 | 0.55 ± 0.06 | 0.41 ± 0.05 |
| Consensus model | 0.86 ± 0.04 | 0.86 ± 0.04 | 0.43 ± 0.04 | 0.34 ± 0.04 |

$q^2$, cross-validation coefficient; $R^2$, squared correlation coefficient; RMSE, root mean squared error; MAE, mean absolute error.

**Table 4:** Statistical coefficients of QSAR models for *dataset 2*

| QSAR Models | Statistical coefficients | | | |
|---|---|---|---|---|
| | $q^2$ | $R^2$ | RMSE | MAE |
| Model 1 | 0.89 ± 0.04 | 0.89 ± 0.03 | 0.3 ± 0.05 | 0.19 ± 0.02 |
| Model 2 | 0.92 ± 0.02 | 0.92 ± 0.02 | 0.25 ± 0.02 | 0.18 ± 0.02 |
| Model 3 | 0.91 ± 0.03 | 0.91 ± 0.02 | 0.27 ± 0.03 | 0.2 ± 0.02 |
| Model 4 | 0.91 ± 0.02 | 0.91 ± 0.02 | 0.27 ± 0.02 | 0.2 ± 0.02 |
| Model 5 | 0.81 ± 0.08 | 0.85 ± 0.05 | 0.39 ± 0.08 | 0.24 ± 0.03 |
| Consensus model | 0.91 ± 0.03 | 0.91 ± 0.03 | 0.26 ± 0.04 | 0.18 ± 0.02 |

$q^2$, cross-validation coefficient; $R^2$, squared correlation coefficient; RMSE, root mean squared error; MAE, mean absolute error.

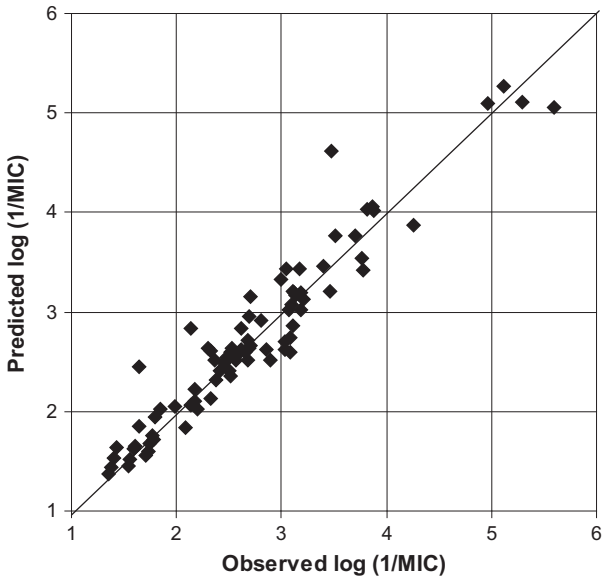


**Figure 2:** Plots of experimental values and predicted values of the consensus QSAR model for *dataset 2*.

liquid (Figure 3) with different activity levels of antimicrobial potential were identified for the synthesis and biological testing.

### *Synthesis of 1,3-dialkylimidazolium ionic liquid*

The following chemicals were used for the synthesis of ionic liquids: imidazole (Shanghai Synnad, China), 1-methylimidazole, 1-butylimidazole, 1-benzylimidazole, 1-allylimidazole, 1-(2-hydroxyethyl)imidazole, N,N-dimethylformamide, methylene chloride, ethyl acetate, hexane (Fluka), 1-bromohexane, 1-bromooctane, 1-bromononane, 1-bromodecane, 1-bromododecane, 1-chlorododecane, 1-bromohexadecane, tetrafluoroboric acid (48% in $H_2O$; Sigma-Aldrich, St. Louis, MO, USA).

1-tetrafluoroethylimidazole was synthesized by following method. To a solution of 13.6 g (0.2 mol) of imidazole in 150 mL of dry THF in 500 mL round-bottom flask, 100 mg of potassium suspended in 2 mL of hexane, was added. After finishing of gas ($H_2$) evolution, the flask was evacuated and, the atmosphere of tetrafluoroethylene was done. The reaction mixture was vigorously stirred in the atmosphere of tetrafluoroethylene at 25–30 °C while adsorption of the gas stopped (about 30–35 h). The solvent was removed at reduced pressure. The residue was taken with 200 mL of ether and washed with water (50 mL) to remove unreacted imidazole. The ether solution was dried with $MgSO_4$. The solvent was distilled off, and the product was distilled in vacuum. Yield 78%, b. p. 50 °C/15 mmHg.

ILs comprising asymmetric 1.3-dialkylimidazolium cations were synthesized according to the methods described in Refs 37,38 (Figure 4).

To obtain water soluble chloride or bromide 1,3-dialkylimidazolium ionic liquids, equimolar mixture of N-substituted imidazole and corresponding halogenoalkane was stirred at 120–140 °C from 2 to 20 h under an argon atmosphere. The obtained viscous liquids were cooled to room temperature and washed three times with hexane-ethyl acetate mixture or neat hexane in order to remove unreacted initial compounds. Solid compounds were recrystallized from hexane-ethyl acetate mixture or from neat hexane. Residual solvent was removed in vacuum 10 mbar at 70–80 °C for 24 h.

Symmetric 1,3-dialkylimidazoliun ILs with chloride or bromide anion were synthesized by following method (Figure 5).

Imidazole (5 g, 0.073 mol) was dissolved in 40 mL of dry N, N-dimethylformamide. Potassium carbonate (11.5 g. 0.08 mol) and corresponding halogenoalkane (0.15 mol) were added to the solution and then the mixture was stirred at 80–120 °C for 20 h. After cooling to room temperature, the mixture was poured into 100 mL of water. The top water immiscible layer of ionic liquid was extracted with methylene chloride (2 × 50 mL) and dried overnight with sodium sulfate. The solvent was removed by distillation, the obtained viscous liquid was purified by washing with ethyl acetate-hexane mixture (3 × 50 mL). If products were solid, they were purified by recrystallization from ethyl acetate-hexane mixture or from neat hexane. Residual solvents were removed in vacuum 10 mbar at 70–80 °C for 24 h.

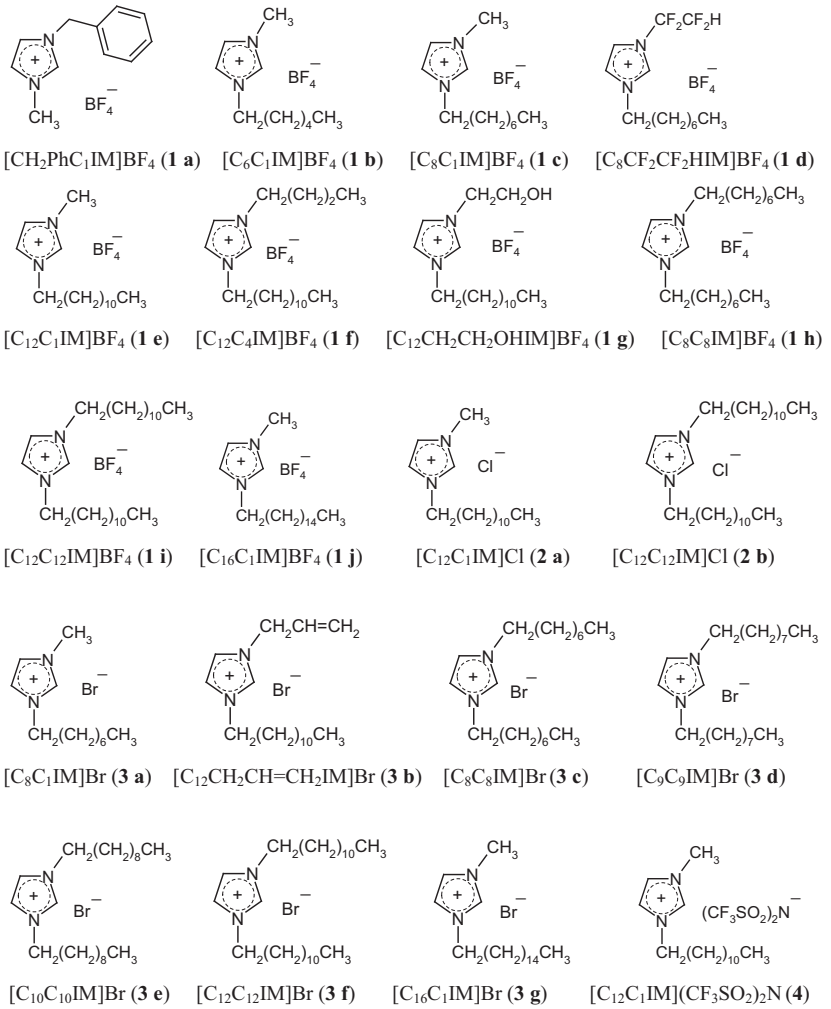


**Figure 3:** Chemical structures of 1,3-dialkylimidazolium ILs.

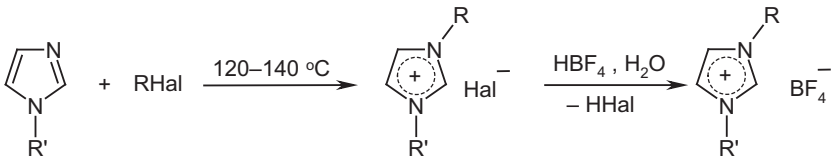


R = $C_6H_{13}$, $C_8H_{17}$, $C_{12}H_{25}$, $C_{16}H_{33}$, $CH_2Ph$ Hal = Cl, Br

R' = $CH_3$, $C_4H_9$, $CH_2CH_2OH$, $CH_2CH{=}CH_2$, $CF_2CF_2H$

**Figure 4:** Synthesis of asymmetric 1,3-dialkylimidazolium ionic liquids.

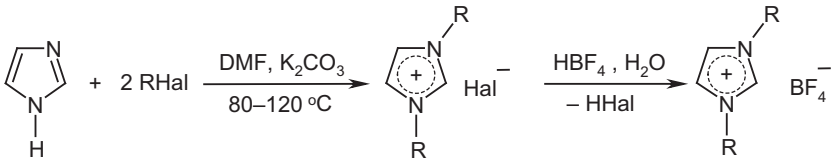


R = $C_8H_{17}$, $C_9H_{19}$, $C_{10}H_{21}$, $C_{12}H_{25}$

Hal = Cl, Br

**Figure 5:** Synthesis of symmetric 1,3-dialkylimidazolium ionic liquids.

To obtain water-immiscible ILs, the corresponding chloride or bromide 1,3-dialkylimidazolium IL was dissolved in water (10 wt%) followed by the addition of tetrafluoroboric acid (~10% molar excess over IL concentration). The formed water-immiscible layer (or semi-solid residue) was extracted with methylene chloride (2 × 50 mL) and dried overnight under sodium sulfate. The solvent was distilled off and the product was dried in vacuum 1 mbar at 70–80 °C for 12 h.

1-benzyl-3-methylimidazolium tetrafluoroborate (**1a**)

m. p. 73–74 °C.

$^1$H NMR (300 MHz, DMSO-$D_6$): $\delta$ = 3.86 (s, 3H, $NCH_3$), 5.42 (s, 2H, $NCH_2$), 7.37–7.42 (m, 5H, $H_{aryl}$), 7.69 (br s, 1H, $C_4$–H), 7.76 (br s, 1H, $C_5$–H), 9.17 (s, 1H, $C_2$–H).

$^{19}$F NMR (188 MHz, DMSO-$D_6$): $\delta$ = −148.4 (s, 4F, $BF_4$).

1-hexyl-3-methylimidazolium tetrafluoroborate (**1b**)

$^1$H NMR (400 MHz, DMSO-$D_6$): $\delta$ = 0.86 (t, 3H, $CH_3$), 1.27 (m, 6H, $(CH_2)_3$), 1.78 (m, 2H, $CH_2$), 3.85 (s, 3H, $NCH_3$), 4.15 (t, 2H, $NCH_2$), 7.68 (br s, 1H, $C_4$–H), 7.75 (br s, 1H, $C_5$–H), 9.07 (s, 1H, $C_2$–H).

$^{19}$F NMR (188 MHz, DMSO-$D_6$): $\delta$ = −147.3 (s, 4F, $BF_4$).

1-octyl-3-methylimidazolium tetrafluoroborate (**1c**)

$^1$H NMR (300 MHz, DMSO-$D_6$): $\delta$ = 0.85 (t, 3H, $CH_3$), 1.25 (m, 10H, $CH_3(CH_2)_5$), 1.78 (m, 2H, $NCH_2CH_2$), 3.85 (s, 3H, $NCH_3$), 4.16 (t, 2H, $NCH_2$), 7.67 (br s, 1H, $C_4$-H), 7.74 (br s, 1H, $C_5$–H), 9.06 (s, 1H, $C_2$–H).

$^{19}$F NMR (188 MHz, DMSO-$D_6$): $\delta$ = −148.8) (s, 4F, $BF_4$).

1-octyl-3-tetrafluoroethylimidazolium tetrafluoroborate (**1d**)

m. p. 49–50 °C.

$^1$H NMR (300 MHz, DMSO-$D_6$): $\delta$ = 0.88 (t, 3H, $CH_3$), 1.29 (m, 10H, $CH_3(CH_2)_5$), 2.52 (m, 2H, $NCH_2CH_2$), 4.30 (t, 2H, $NCH_2$), 7.15–7.32 (m, 1H, $CF_2H$), 8.17 (br s, 1H, $C_4$–H), 8.32 (br s, 1H, $C_5$–H), 10.04 (s, 1H, $C_2$–H).

$^{19}$F NMR (188 MHz, DMSO-$D_6$): $\delta$ = −148.7 (s, 4F, $BF_4$), −137.31 to −137.53 (d t, 2F, $CF_2H$), −99.51 (t, 2F, $CF_2$).

1-dodecyl-3-methylimidazolium tetrafluoroborate (**1e**)

m. p. 27–28 °C.

$^1$H NMR (300 MHz, DMSO-$d_6$): $\delta$ = 0.84 (t, 3H, $CH_3$), 1.25–1.31 (m, 18H, $CH_3(CH_2)_9$), 1.85 (m, 2H, $NCH_2CH_2$), 3.84 (s, 3H, $NCH_3$), 4.15 (t, 2H, $NCH_2$, J = 7.2 Hz), 7.68 (br s, 1H, $C_4$–H), 7.75 (br s, 1H, $C_5$–H), 9.09 (s, 1H, $C_2$–H).

$^{19}$F NMR (188 MHz, DMSO-$d_6$): $\delta$ = −148.2 (s, 4F, $BF_4$).

1-dodecyl-3-butylimidazolium tetrafluoroborate (**1f**)

$^1$H NMR (300 MHz, $CDCl_3$): $\delta$ = 0.87–0.95 (m, 6H, $CH_3$), 1.24 (m, 20H, $CH_3(CH_2)_{10}$), 1.87 (m, 4H, $NCH_2CH_2$), 4.21 (m, 4H, $NCH_2$), 7.39 (br s, 1H, $C_4$–H), 7.43 (br s, 1H, $C_5$–H), 8.87 (s, 1H, $C_2$–H).

$^{19}$F NMR (188 MHz, $CDCl_3$): $\delta$ = −151.7 (s, 4F, $BF_4$).

1-dodecyl-3-(2-hydroxyethyl)imidazolium tetrafluoroborate (**1g**)

$^1$H NMR (300 MHz, DMSO-$D_6$): $\delta$ = 0.83 (t, 3H, $CH_3$), 1.23 (m, 18H, $CH_3(CH_2)_9$), 1.79 (m, 2H, $NCH_2CH_2$), 3.49 (br s, 1 H, OH), 3.75 (m, 2H, $NCH_2CH_2OH$), 4.17-4.22 (m, 4 H, $NCH_2$), 7.69–7.71 (m, 2H, $C_4$–H, $C_5$–H), 9.07 (s, 1H, $C_2$–H).

$^{19}$F NMR (188 MHz, DMSO-$D_6$): $\delta$ = −148.6 (s, 4F, $BF_4$).

1,3-dioctylimidazolium tetrafluoroborate (**1h**)

$^1$H NMR (300 MHz, $CDCl_3$): $\delta$ = 0.84–0.86 (m, 6H, $CH_3$), 1.25–1.31 (m, 20H, $CH_3(CH_2)_5$), 1.87 (m, 4H, $NCH_2CH_2$), 4.18–4.22 (m, 4H, $NCH_2$), 7.4 (m, 2H, $C_4$–H, $C_5$–H), 8.86 (s, 1H, $C_2$–H).

$^{19}$F NMR (188 MHz, $CDCl_3$): $\delta$ = −151.6 (s, 4F, $BF_4$).

1,3-didodecylimidazolium tetrafluoroborate (**1i**)

m. p. 52–53 °C.

$^1$H NMR (400 MHz, DMSO-$D_6$): $\delta$ = 0.85 (t, 6H, $CH_3$), 1.23–1.27 (m, 36H, $CH_3(CH_2)_9$), 1.79 (m, 4H, $NCH_2CH_2$), 4.18 (t, 4H, $NCH_2$), 7.84 (m, 2H, $C_4$–H, $C_5$–H), 9.42 (s, 1H, $C_2$–H).

$^{19}$F NMR (188 MHz, DMSO-$D_6$): $\delta$ = –148.4 (s, 4F, $BF_4$).

1-hexadecyl-3-methylimidazolium tetrafluoroborate (**1j**)

m. p. 54–55 °C.

$^1$H NMR (300 MHz, DMSO-$D_6$): $\delta$ = 0.85 (t, 3H, $CH_3$), 1.24 (m, 26H, $CH_3(CH_2)_{13}$), 1.78 (m, 2H, $NCH_2CH_2$), 3.84 (s, 3H, $NCH_3$), 4.14 (t, 2H, $NCH_2$), 7.69 (br s, 1H, $C_4$-H, 7.76 (br s, 1H, $C_5$-H), 9.08 (s, 1H, $C_2$-H).

$^{19}$F NMR (188 MHz, DMSO-$D_6$): $\delta$ = -148.2 (s, 4F, $BF_4$).

1-dodecyl-3-methylimidazolium chloride (**2a**)

m. p. 46-47 °C.

$^1$H NMR (300 MHz, DMSO-$D_6$): $\delta$ = 0.85 (t, 3H, $CH_3$), 1.24 (m, 18H, $CH_3(CH_2)_9$), 1.79 (m, 2H, $NCH_2CH_2$), 3.91

(s, 3H, $NCH_3$), 4.22 (t, 2H, $NCH_2$), 7.84 (br s, 1H, $C_4$-H), 7.92 (br s, 1H, $C_5$-H), 9.57 (s, 1H, $C_2$-H).

1,3-didodecylimidazolium chloride (**2b**)

m. p. 49-50 °C.

$^1$H NMR (300 MHz, DMSO-$D_6$): $\delta$ = 0.85 (t, 6H, $CH_3$), 1.24-1.27 (m, 36H, $CH_3(CH_2)_9$), 1.79 (m, 4H, $NCH_2CH_2$), 4.18 (t, 4H, $NCH_2$), 7.84 (m, 2H, $C_4$-H, $C_5$-H), 9.32 (s, 1H, $C_2$-H).

1-octyl-3-methylimidazolium bromide (**3a**)

$^1$H NMR (300 MHz, DMSO-$D_6$): $\delta$ = 0.86 (t, 3H, $CH_3$), 1.24 (m, 10H, $CH_3(CH_2)_5$), 1.79 (m, 2H, $NCH_2CH_2$), 3.90 (s, 3H, $NCH_3$), 4.20 (t, 2H, $NCH_2$), 7.85 (br s, 1H, $C_4$-H), 7.93 (br s, 1H, $C_5$-H), 9.59 (s, 1H, $C_2$-H).

1-dodecyl-3-allylimidazolium bromide (**3b**)

$^1$H NMR (300 MHz, $CDCl_3$): $\delta$ = 0.88 (t, 3H, $CH_3$), 1.25 (m, 18H, $CH_3(CH_2)_9$), 1.94 (m, 2H, $NCH_2CH_2$), 4.36 (t, 2H, $NCH_2$), 5.08 (d, 2H, $NCH_2CH{=}CH_2$), 5.46 (m, 2H, $NCH_2CH{=}CH_2$), 6.08 (m, 1H, $NCH_2CH{=}CH_2$), 7.64 (br s, 1H, $C_4$-H), 7.68 (br s, 1H, $C_5$-H), 10.35 (s, 1H, $C_2$-H).

1,3-dioctylimidazolium bromide (**3c**)

$^1$H NMR (400 MHz, DMSO-$D_6$): $\delta$ = 0.85 (m, 6H, $CH_3$), 1.25 (m, 20H, $CH_3(CH_2)_5$), 1.79 (m, 4H, $NCH_2CH_2$), 4.17 (t, 4H, $NCH_2$), 7.83 (m, 2H, $C_4$-H, $C_5$-H), 9.26 (s, 1H, $C_2$-H).

1,3-dinonylimidazolium bromide (**3d**)

$^1$H NMR (300 MHz, $CDCl_3$): $\delta$ = 0.86 (t, 6H, $CH_3$), 1.24-1.3 (m, 24H, $CH_3(CH_2)_6$), 1.85 (m, 4H, $NCH_2CH_2$), 4.17-4.21 (t, 4H, $NCH_2$), 7.42 (m, $C_4$-H, $C_5$-H), 8.9 (s, 1H, $C_2$-H).

1,3-didecylimidazolium bromide (**3e**)

$^1$H NMR (300 MHz, $CDCl_3$): $\delta$ = 0.84 (t, 6H, $CH_3$), 1.26 (m, 28H, $CH_3(CH_2)_7$), 1.85 (m, 4H, $NCH_2CH_2$), 3.93(t, 4H, $NCH_2$), 7.35 (m, $C_4$-H, $C_5$-H), 8.74 (s, 1H, $C_2$-H).

1,3-didodecylimidazolium bromide (**3f**)

m. p. 40-41 °C.

$^1$H NMR (300 MHz, DMSO-$D_6$): $\delta$ = 0.85 (t, 6H, $CH_3$), 1.26 (m, 36H, $CH_3(CH_2)_9$), 1.79 (m, 4H, $NCH_2CH_2$), 4.18 (t, 4H, $NCH_2$), 7.83 (m, 2H, $C_4$-H, $C_5$-H), 9.31 (s, 1H, $C_2$-H).

1-hexadecyl-3-methylimidazolium bromide (**3 g**)

m. p. 63-64 °C.

**Table 5:** Growth inhibition of *B. subtilis* and *Ps. aeruginosa* by an imidazolium-based ILs. The diameters of inhibition zones are given in millimeters.

| | Content on a disc | | |
|---|---|---|---|
| ILs | $1{\cdot}10^{-7}$ mole | *Ps. aeruginosa* | *B. subtilis* |
| $[CH_2PhC_1IM]BF_4$ | 7.7[a] | na | 10 |
| **1 a** | 0.8[b] | na | na |
| $[C_6C_1IM]BF_4$ | 7.9 | na | na |
| **1 b** | 0.8 | na | na |
| $[C_8C_1IM]BF_4$ | 7.1 | na | 10 |
| **1 c** | 0.7 | na | na |
| $[C_8CF_2CF_2HIM]BF_4$ | 5.4 | na | na |
| **1 d** | 0.5 | na | na |
| $[C_{12}C_1IM]BF_4$ | 5.9 | 29 | 33 |
| **1 e** | 0.6 | 17 | 20 |
| $[C_{12}C_4IM]BF_4$ | 5.3 | 20 | 26 |
| **1 f** | 0.5 | 15 | 18 |
| $[C_{12}CH_2CH_2OHIM]BF_4$ | 5.4 | 25 | 26 |
| **1 g** | 0.5 | 11 | 12 |
| $[C_8C_8IM]BF_4$ | 5.4 | 38 | 38 |
| **1 h** | 0.5 | 23 | 25 |
| $[C_{12}C_{12}IM]BF_4$ | 4.1 | 15 | 13 |
| **1 i** | 0.4 | na | na |
| $[C_{16}C_1IM]BF_4$ | 5.1 | 8 | 10 |
| **1 g** | 0.5 | na | na |
| $[C_{12}C_1IM]Cl$ | 7.0 | 31 | 28 |
| **2 a** | 0.7 | 24 | 15 |
| $[C_{12}C_{12}IM]Cl$ | 4.5 | 10 | 10 |
| **2 b** | 0.5 | na | Na |
| $[C_8C_1IM]Br$ | 7.3 | 12 | na |
| **3 a** | 0.7 | na | na |
| $[C_{12}CH_2CH{=}CH_2IM]Br$ | 5.6 | 27 | 28 |
| **3 b** | 0.6 | 19 | 20 |
| $[C_8C_8IM]Br$ | 5.4 | 32 | 34 |
| **3 c** | 0.5 | 27 | 24 |
| $[C_9C_9IM]Br$ | 5.0 | 27 | 19 |
| **3 d** | 0.5 | 20 | 14 |
| $[C_{10}C_{10}IM]Br$ | 4.7 | 12 | 13 |
| **3 e** | 0.5 | na | na |
| $[C_{12}C_{12}IM]Br$ | 4.1 | 11 | 8 |
| **3 f** | 0.4 | na | na |
| $[C_{16}C_1IM]Br$ | 5.2 | 8 | 12 |
| **3 g** | 0.5 | na | na |
| $[C_{12}C_1IM](CF_3SO_2)_2N$ | 3.8 | 20 | 23 |
| **4** | 0.4 | 10 | 11 |

na, not active.
[a]The content of moles on the disc corresponds to concentration of compounds 1%.
[b]The content of moles on the disc corresponds to concentration of compounds 0.1%.

$^1$H NMR (300 MHz, DMSO-$D_6$): $\delta$ = 0.86 (t, 3H, $CH_3$), 1.24 (m, 26H, $CH_3(CH_2)_{13}$), 1.79 (m, 2H, $NCH_2CH_2$), 3.90 (s, 3H, $NCH_3$), 4.21 (t, 2H, $NCH_2$), 7.85 (br s, 1H, $C_4$-H,), 7.92 (br s, 1H, $C_5$-H), 9.59 (s, 1H, $C_2$-H).

1-dodecyl-3-methylimidazolium bis(trifluoromethylsulfonyl) imide (**4**)

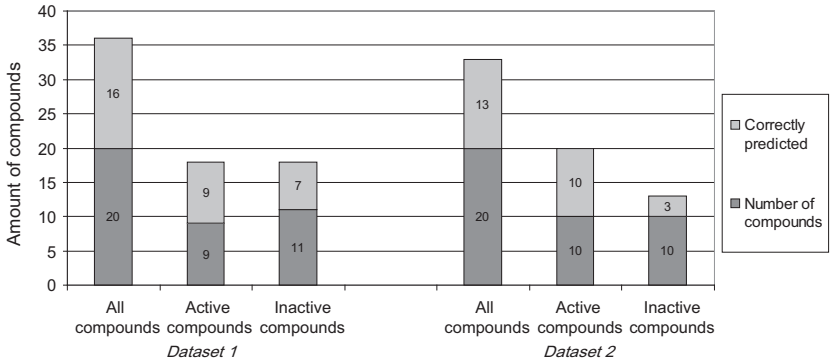


**Figure 6:** Antibacterial activity prediction of 1,3-dialkylimidazolium ILs for *dataset 1* and *dataset 2* using classification QSAR models.

**Table 6:** ILs Predicted activity via regression QSAR models for *dataset 1* and *dataset 2*

| | Predicted activity for *dataset 1.* log(1/MIC) | | | | | | Predicted activity for *dataset 2.* log(1/MIC) | | | | | |
|---|---|---|---|---|---|---|---|---|---|---|---|---|
| ILs | M1 | M2 | M3 | M4 | M5 | Mean | M1 | M2 | M3 | M4 | M5 | Mean |
| 1a | 2.6 | 2.7 | 2.5 | 3.1 | 3.6 | 2.9 ± 0.4 | 2.7 | 2.1 | 2.5 | 2.1 | 2.6 | 2.4 ± 0.25 |
| 1b | 2.8 | 2.8 | 2.7 | 3.0 | 3.6 | 3.4 ± 0.32 | 2.3 | 2.2 | 2.4 | 2.5 | 2.6 | 2.4 ± 0.26 |
| 1c | 3.0 | 3.0 | 3.0 | 3.1 | 3.6 | 3.2 ± 0.25 | 2.9 | 2.7 | 2.8 | 2.9 | 3.0 | 2.9 ± 0.1 |
| 1d | 5.0 | 3.1 | 3.0 | 3.0 | 5.2 | 3.9 ± 1.0 | 4.8 | 2.7 | 2.8 | 2.2 | 5.2 | 3.5 ± 1.21 |
| 1e | 4.1 | 4.4 | 4.5 | 4.2 | 4.3 | 4.3 ± 0.14 | 3.0 | 3.1 | 3.1 | 3.0 | 3.0 | 3.1 ± 0.05 |
| 1f | 4.7 | 4.8 | 5.1 | 5.3 | 4.3 | 4.9 ± 0.34 | 3.1 | 3.2 | 3.4 | 3.9 | 3.0 | 3.3 ± 0.31 |
| 1g | 4.5 | 4.4 | 3.8 | 3.9 | 4.3 | 4.2 ± 0.28 | 3.1 | 4.7 | 4.0 | 4.6 | 3.0 | 3.9 ± 0.40 |
| 1h | 4.7 | 4.9 | 5.2 | 5.4 | 4.3 | 4.9 ± 0.38 | 3.1 | 3.3 | 3.4 | 3.9 | 3.0 | 3.4 ± 0.31 |
| 1i | 5.2 | 5.4 | 5.4 | 5.7 | 4.3 | 5.2 ± 0.48 | 3.2 | 3.5 | 3.3 | 4.2 | 3.0 | 3.5 ± 0.41 |
| 1j | 4.9 | 4.9 | 5.2 | 4.9 | 4.3 | 4.9 ± 0.29 | 3.1 | 3.2 | 3.3 | 3.2 | 3.0 | 3.2 ± 0.1 |
| 2a | 4.1 | 4.4 | 4.5 | 4.2 | 4.3 | 4.3 ± 0.14 | 3.0 | 3.1 | 3.1 | 3.0 | 3.0 | 3.1 ± 0.05 |
| 2b | 5.2 | 5.4 | 5.4 | 5.7 | 4.3 | 5.2 ± 0.48 | 3.2 | 3.5 | 3.3 | 4.2 | 3.0 | 3.5 ± 0.40 |
| 3a | 3.0 | 3.0 | 3.0 | 3.1 | 3.6 | 3.2 ± 0.23 | 2.8 | 2.7 | 2.8 | 2.8 | 2.6 | 2.8 ± 0.1 |
| 3b | 4.4 | 4.6 | 4.9 | 4.5 | 4.3 | 4.56 ± 0.2 | 3.3 | 3.2 | 3.3 | 3.3 | 3.0 | 3.2 ± 0.1 |
| 3c | 4.7 | 4.9 | 5.2 | 5.4 | 4.3 | 4.9 ± 0.38 | 3.1 | 3.3 | 3.4 | 3.9 | 3.0 | 3.4 ± 0.3 |
| 3d | 4.9 | 5.2 | 5.4 | 5.4 | 4.3 | 5.0 ± 0.41 | 3.2 | 3.5 | 3.4 | 4.0 | 3.0 | 3.4 ± 0.33 |
| 3e | 5.0 | 5.3 | 5.7 | 5.5 | 4.3 | 5.17 ± 0.5 | 3.2 | 3.4 | 3.4 | 4.1 | 3.0 | 3.5 ± 0.37 |
| 3f | 5.2 | 5.4 | 5.4 | 5.7 | 4.3 | 5.2 ± 0.48 | 3.2 | 3.5 | 3.3 | 4.2 | 3.0 | 3.5 ± 0.41 |
| 3g | 4.9 | 4.9 | 5.2 | 4.9 | 4.3 | 4.88 ± 0.3 | 3.1 | 3.2 | 3.3 | 3.2 | 3.0 | 3.2 ± 0.1 |
| 4 | 4.1 | 4.4 | 4.5 | 4.2 | 4.3 | 4.3 ± 0.14 | 3.0 | 3.1 | 3.1 | 3.0 | 3.0 | 3.0 ± 0.05 |

M1, QSAR model number 1.

$^1$H NMR (300 MHz, DMSO-$D_6$): $\delta$ = 0.87 (t, 3H, $CH_3$), 1.25 (m, 18H, $CH_3(CH_2)_9$), 1.85 (m, 2H, $NCH_2CH_2$), 3.93 (s, 3H, $NCH_3$), 4.15 (t, 2H, $NCH_2$), 7.31 (br s, 1H, $C_4$-H), 7.34 (br s, 1H, $C_5$-H), 8.72 (s, 1H, $C_2$-H).

$^{19}$F NMR (188 MHz, DMSO-$D_6$): $\delta$ = -79.92 (s, 6F, $CF_3$).

## *Biological testing*

The antibacterial activities of the 20 imidazolium-based ILs (Figure 3) against *B. subtilis* and *Ps. aeruginosa* are shown in Table 5.

The data presented in Table 5 indicate high antibacterial activity of both water soluble and water immiscible asymmetric 1,3-dialkylimidazolium ionic liquids, comprising at least one C12-alkyl radical (compounds **1e**, **1f**, **1g, 2a, 3b, 4),** as well as symmetric 1,3-dialkylimidazolium ionic liquids, comprising shorter alkyl chains of C8 and C9 carbon atoms (**1h**, **3c**, **3d**).

Experimental results and results of prediction by means of the classification and regression QSAR models were compared.

Figure 6 presents the data about coincidence between the predicted activity of classification QSAR models and the real activity of the studied compounds.

Classification QSAR models correctly predicted the antibacterial activity of 80% of compounds for *dataset 1*. The 9 ILs **1e**, **1f**, **1g**, **1h**, **2a**, **3b**, **3c**, **3d,** and **4** were predicted as active against *B. subtilis*, which coincides with the results of biological testing. 11 compounds were predicted as inactive, but seven of them (64%) were really inactive.

For *dataset 2,* about 65% of compounds were predicted correctly by classification QSAR models. The 10 ILs **1e**, **1f**, **1g**, **1h**, **1i**, **2a**, **3b**, **3c, 3d,** and **4** were predicted as active against *Ps. aeruginosa* that coincides with the results of biological testing. 10 compounds were predicted as inactive, but 3 (34%) were really inactive.

The data presented in Table 6 show the predicted level of ILs activity via regression QSAR models for *dataset 1* and *dataset 2.*

Compounds **1f**, **1h**, **1i**, **1j**, **2b**, **3c**, **3d**, **3e,** and **3f** were predicted as the most active against *B. subtilis.* The results of biological screening of the imidazolium ILs confirmed the QSAR predictions for ILs **1f**, **1h**, **3c**, **3d**, **3e** (55%).

Compounds **1d, 1g**, **1h, 1i, 2b**, **3c**, **3d**, **3e,** and **3f** were with high predicted activity against *Ps. aeruginosa.* The real biological activity was demonstrated by compounds ILs **1g**, **1h**, **3c**, **3d** (45%).

## Conclusions

Classification and regression predictive QSAR models of imidazolium-based ionic liquids antibacterial activity were created. The developed classification QSAR models were a good predictive quality with accuracy 83% and 88% for *dataset 1* and *dataset 2* respectively. All the created regression QSAR models have a good predictive quality too with $q^2$ ranged from 0.77 to 0.86 for *dataset 1* and ranged from 0.81 to 0.92 for *dataset 2.* It means that the developed QSAR models can be used to search for a new active antibacterial imidazolium-based ionic liquids as potential antimicrobial agents.

The antibacterial activity of 20 synthesized compounds of 1,3-dialkylimidazolium ionic liquid with different level of predictive activity was evaluated.

The predictive ability of classification models was better than ability of regression models. The coincidence between the predicted activity of classification QSAR models and the real activity of the studied ILs as 80% for *dataset 1* and 65% for *dataset 2* was determined. The coincidence between the predicted activity of regression QSAR models and the real activity of the studied ILs was lower than 55%. Therefore, it can be better to use classification models of evaluation of activity of imidazolium-based ionic liquids as potential antibacterial agents.

## References


1. Allegranzi B., Nejad S.B., Combescure C., Graafmans W., Attar H., Donaldson L., Pittet D. (2011) Burden of endemic health-care-associated infection in developing countries: systematic review and meta-analysis. Lancet;377:228–241.
2. Kaali P., Strömberg E., Karlsson S. (2011) Prevention of biofilm associated infections and degradation of polymeric materials used in biomedical applications. In: Laskovski A.N., editor. Biomedical Engineering, Trends in Material Science, Chapter 22. Rijeka: In Tech, p. 513–541.
3. Gilbert P., Moore L.E. (2005) Cationic antiseptics: diversity of action under a common epithet. J Appl Microbiol;99:703–715.
4. Russel A.D. (2003) Biocide use and antibiotic resistance: the relevance of laboratory findings to clinical and environmental situations. Lancet Infect Dis;3:794–803.
5. Russel A.D. (1986) Chlorhexidine: antibacterial action and bacterial resistance. Infection;14:212–215.
6. Fazlara A., Ekhtelat M. (2012) The disinfectant effects of benzalkonium chloride on some important foodborne pathogens. J Agric Environ Sci;12:23–29.
7. Mc Cay P.H., Ocampo-Sosa A.A., Fleming G.T. (2010) Effect of subinhibitory concentrations of benzalkonium chloride on the competitiveness of Pseudomonas aeruginosa grown in continuous culture. Microbiology;156:30–38.
8. Welton T. (1999) Room-Temperature Ionic Liquids. Solvents for Synthesis and Catalysis. Chem Rev;99:2071–2084.
9. Hong K., Zhang H., Mays J., Visser A., Brazel C., Holbrey J., Reichert W., Rogers R. (2002) Conventional free radical polymerization in room temperature ionic liquids: a green approach to commodity polymers with practical advantages. Chem Commun;13:1368–1369.
10. Naushad M., Alothman Z., Khan A., Ali M. (2012) Effect of ionic liquid on activity, stability, and structure of enzymes: a review. Int J Biol Macromol;51:555–560.
11. Arning J., Stolte S., Boschen A., Stock F., Pitner W.-R., Welz-Biermann U., Jastorff B., Ranke J. (2008) Qualitative and quantitative structure activity relationships for the inhibitory effects of cationic head groups, functionalized side chains and anions of ionic liquids on acetylcholinesterase. Green Chem;10:47–58.
12. Shamshina J., Barber P., Rogers R. (2013) Ionic liquids in drug delivery. Expert Opin Drug Deliv;10:1367–1381.
13. Gilmore B.F., Earle M.J. (2011) Development of ionic liquid biocides against microbial biofilm. Chim Oggi;29:50–53.
14. Pernak J., Sobaszkiewicz K., Mirska I. (2003) Anti-microbial activities of ionic liquids. Green Chem;5:52–56.
15. Demberelnyamba D., Kim K., Choi S., Park S., Lee H., Kim C., Yoo I. (2004) Synthesis and antimicrobial properties of imidazolium and pyrrolidinium salts. Bioorg Med Chem;12:853–857.
16. Docherty K., Kulpa C. (2005) Toxicity and antimicrobial activity of imidazolium and pyridinium ionic liquids. Green Chem;7:185–189.
17. Iwai N., Nakauama K., Kitazume T. (2011) Antibacterial activities of imidazolium, pyrrolidinium and piperidinium salts. Bioorg Med Chem Lett;21:1728–1729.

18. Yu Y., Nie Y. (2011) Toxicity and Antimicrobial Activities of Ionic Liquids with Halogen Anion. J Environ Prot;2:298–303.
19. Borowiecki P., Milner-Krawczyk M., Brzezin′ska D., Wielechowska M., Plenkiewicz J. (2013) Synthesis and Antimicrobial Activity of Imidazolium and Triazolium Chiral Ionic Liquids. Eur J Org Chem;2013:712–720.
20. Mester P., Wagner M., Rossmanith P. (2015) Antimicrobial effects of short chained imidazolium based ionic liquids – influence of anion chaotropicity. Ecotoxicol Environ Saf;111:96–101.
21. Pendleton J.N., Gilmore B.F. (2015) The antimicrobial potential of ionic liquids: A source of chemical diversity for infection and biofilm control. Int J Antimicrob Agents;46:131–139.
22. Luczak J., Jungnickel C., Laska I., Stolte S., Hupka J. (2010) Antimicrobial and surface activity of 1-alkyl-3-methyl imidazolium derivatives. Green Chem;12:593–601.
23. Cornellas A., Perez L., Comelles F., Ribosa I., Manresa A. (2011) Self-aggregation and antimicrobial activity of imidazolium and pyridinium based ionic liquids in water solutions. J Colloid Interface Sci;355:164–171.
24. Venkata Nancharaiah Y., Kiran Kumar Reddy G., Lalithamanasa P., Venugopalan V.P. (2012) The ionic liquid 1-alkyl-3-methylimidazolium demonstrates comparable antimicrobial and antibiofilm behavior to a cationic surfactant. Biofouling;28:1141–1149.
25. Tetko I.V. (2008) Associative neural network. Methods Mol Biol;458:185–202.
26. Tetko I.V. (2002) Associative neural network. Neural Process Lett;16:187–199.
27. Vorberg S., Tetko I.V. (2014) Modeling the Biodegradability of Chemical Compounds Using the Online Chemical Modeling Environment (OCHEM). Molecular Informat;33:73–85.
28. Livingston F. (2005) Implementation of Breiman's random forest machine learning algorithm. ECE591Q Mach Learn J Pap;1–13.
29. Breiman L. (2001) Random forests. Mach Learn;45:5–32.
30. Tetko I.V., Tanchuk V.Yu. (2002) Application of associative neural networks for prediction of lipophilicity in ALOGPS 2.1 program. J Chem Inf Comput Sci;42:1136–1145.
31. Hall L.H., Kier L.B., Brown B.B. (1995) Molecular Similarity Based on Novel Atom-Type Electrotopological State Indices. J Chem Inf Comput Sci;35:1074–1080.
32. Sushko I., Pandey A.K., Novotarskyi S. (2011) Online Chemical Modeling Environment (OCHEM): Web Platform for Data Storage. Model Development and Publishing of Chemical Information. J Cheminform;3:20.
33. Tetko I.V., Baskin I.I., Varnek A.. (2008) Tutorial on machine learning. Part 2. Descriptor selection bias. In: Strasbourg summer school on chemoinformatics: cheminfoS3. Obernai. https://www.researchgate.net/publication/236651951_Tutorial_on_Machine_Learning_Part_2_Descriptor_Selection_Bias (accessed 5 August 2015)
34. Mahobia N.K., Patel R.D., Sheikh N.W., Singh S.K., Mishra A., Dhardubey R. (2010) Validation Method Used In Quantitative Structure Activity Relationship. Der Pharm Chem;2:260–271.
35. Tetko I.V., Sushko I., Pandey A.K., Zhu H., Tropsha A., Papa E., Oberg T., Todeschini R., Fourches D., Varnek A. (2008) Critical assessment of QSAR models of environmental toxicity against Tetrahymena pyriformis: focusing on applicability domain and overfitting by variable selection. J Chem Inf Model;48:1733–1746.
36. Bauer A., Kirby W., Sherris J., Turck M. (1966) Antibiotic susceptibility testing by a standardized single disk method. Am J Clin Pathol;45:493–496.
37. Dzyuba S.V., Bartsch R.A. (2001) Efficient synthesis of 1-alkyl(aralkyl)-3-methyl(ethyl)imidazolium halides: Precursors for room-temperature ionic liquids. J Heterocycl Chem;38:265–268.
38. Rogalsky S., Fatyeyeva K., Lyoshina L., Tarasiuk O., Bulko O., Lobok S. (2014) Antimicrobial properties and thermal stability of polycarbonate modified with 1-alkyl-3-methylimidazolium tetrafluoroborate ionic liquids. J Appl Polym Sci;131:40050.

## Notes

[a]https://ochem.eu/
[b]Adriana.Code web-page. http://www.molecularnetworks.com/products/adrianacode (accessed Dec4. 2010).
[c]http://www.talete.mi.it/products/dragon_description.htm/ (Accessed June 1. 2015).
[d]ChemAxon. https://www.chemaxon.com/ (Accessed May 1. 2015).
[e]http://docs.ochem.eu/display/MAN/OCHEM+Introduction.
[f]http://docs.ochem.eu/display/MAN/Statistical+parameters
[g]http://docs.ochem.eu/display/MAN/Applicability+domain+assessment
[h]https://www.molecular networks.com/products/corina (Accessed May 1. 2015)